

# Vortex scenario and bubble generation in a cylindrical cavity with rotating top and bottom

Valery L. Okulov<sup>1</sup>, Jens N. Sørensen<sup>\*</sup>, Lars K. Voigt

*Department of Mechanical Engineering, Technical University of Denmark, DK-2800 Kongens Lyngby, Denmark*

Received 2 September 2003; received in revised form 13 April 2004; accepted 2 June 2004

Available online 28 July 2004

---

## Abstract

The creation of recirculation bubbles in a steady, viscous flow in a cylindrical cavity with co-rotating top and bottom is investigated numerically. By varying the Reynolds number and the aspect ratio of the cylinder various axial-symmetric flow regimes are studied. It is observed that the topology of re-circulating vortex structures is associated with a change in helical symmetry of the vortex lines. The computations show that symmetry changes take place at increasing Reynolds numbers and that flow reversal on the center axis is associated with a growth of the twist parameter of the vortex lines. For all studied flow cases, independent of aspect ratio and Reynolds number, it was observed that the twist parameter of the central vortex attains a threshold value of  $\mathbf{K} \cong 0.6$  at the point where flow reversal takes place.

© 2004 Elsevier SAS. All rights reserved.

**Keywords:** Swirl flows; Vortex breakdown; Helical symmetry

---

## List of notations

$2\pi l$	pitch of vortex lines (m)
$H$	height of a cylinder (m)
$R$	radius of a cylinder (m)
$Re$	Reynolds number
$(r, \theta, z)$	cylindrical coordinate system (m, rad, m)
$p$	dimensionless local helical pitch of vortex lines
$(u_r, u_\theta, u_z)$	velocity components (m/s)

## Greek letters

$\mathbf{K} = 1/p$	dimensionless local twist parameter of vortex lines
$\Omega$	angular velocities (1/s)
$\nu$	kinematics viscosity of a fluid ( $\text{m}^2/\text{s}$ )
$\omega_r$	radial component of a vorticity (1/s)

---

<sup>\*</sup> Corresponding author. Tel.: +45-45-25-43-00; fax: +45-45-93-06-63.  
E-mail address: [jns@mek.dtu.dk](mailto:jns@mek.dtu.dk) (J.N. Sørensen).

<sup>1</sup> Current address: Institute of Thermophysics, SB RAS, Lavrentyev Ave. 1, Novosibirsk, 630090, Russia.

$\omega_\theta$	azimuthal component of a vorticity (1/s)
$\omega_z$	axial component of a vorticity (1/s)
$\psi$	stream function ( $\text{m}^2/\text{s}$ )

## 1. Introduction

Swirling flows may under certain conditions be subject to abrupt changes associated with flow reversal. This phenomenon, usually referred to as vortex breakdown, is characterized by a change in flow topology where the flow develops a characteristic structure of bubble, spiral or double-helix shape, and a change in the distribution of axial velocity, from a jet-like profile before breakdown to a wake-like profile after breakdown (see [1,2]). A feature of vortex breakdown, discovered and analyzed by Okulov and co-workers [3–5], is the existence of a transition from a right-handed to a left-handed helical vortex structure, that both exist under the same integral flow parameters (i.e. under the same flow rate, circulation, angular and axial momentum and energy). Comparing this theory with a large number of experiments has revealed that vortex breakdown always is associated with a change in helical symmetry from a right-handed vortex structure to a left-handed one. The difference between vortex structures with right- and left-handed helical symmetry implies different signs of torsion or local helical pitch of the vortex lines. The right-handed helical structures induce a jet-like profile of axial velocity and the left-handed helical structures induce a wake-like one, which may be subject to flow reversal on the axis [3,6]. This theory, however, only connects the basic flow features before and after breakdown, whereas it does not explain how the change in helical symmetry takes place. The main objective of the present study is to analyze in detail how the change in helical symmetry of the vortex lines takes place in a well-defined paraxial flow with vortex breakdown. Unfortunately there is no direct way of predicting vorticity fields experimentally. Consequently, in the present work direct numerical simulations were used to establish the necessary data. To simplify the numerical task, in particular with respect to inflow and outflow boundary conditions, a relatively simple flow configuration was established in which a swirling flow was generated by letting the end-walls of a closed cylinder rotate with constant angular velocity.

Swirl flows in a closed cylinder of the basic configuration with one fixed and one rotating cover have been widely studied. The various flow regimes observed in this system are characterized by the appearance of recirculation zones referred to as bubbles, with weak reverse axial flow along the axis. This unique flow phenomenon was first observed experimentally [7–10] and computational results [11–14] have later confirmed most of the experimentally observed findings. Numerical axisymmetric simulations not only predict correctly the onset of reverse flow but also reproduce the location, the size, and the number of bubbles visualized in experiments.

A fundamental aspect of this flow is the question of how the basic state (steady and axisymmetric) breaks the symmetry and becomes unsteady and/or three-dimensional. This problem has in numerous studies been considered by both two- and three-dimensional analyses (see e.g. [15–21]). An important results of these analyses is that the creation of recirculation bubbles in a system with one rotating disk is not associated with an instability, but takes place as a smooth topological change of the steady flow [14,18]. For this reason, in order to understand the basic mechanisms underlying vortex breakdown, the present study only deals with steady and axisymmetric flow cases.

In an earlier numerical study by one of the authors [22], the basic cavity with one rotating cover was used to verify that the vortex lines past a re-circulating bubble change helicity from a right- to a left-handed helical vortex structure. In this case the structures of the analyzed vortex tubes were very complex and deformed, hence it was not the most suitable object for studying the relation between changes in helical symmetry and vortex breakdown. In contrast to this, using a cavity flow with two co-rotating covers, as in the present work, gives a very clear evidence that the appearance of re-circulating bubbles are directly linked to a change in the helical structure of the vortex lines. Note that the fluid motion in a cylinder where swirl is generated by rotating both end-covers (Fig. 1) already has proved to be useful for the study of re-circulating bubbles in swirl flows [23–26]. A full-scale topological classification of different flow patterns by Brøns et al. [27] was devoted to the case of a flow with rotating bottom and a free surface. In the case of a flat, i.e. stress-free, surface this corresponds to a symmetric case with a cylinder of double height where the swirl is generated by rotating both the bottom and the top lid with the same angular velocity. The topological apparatus, developed for axisymmetric swirl flow by Brøns [28], was used systematically to extract features of the flow patterns obtained from numerical simulations to construct the bifurcation diagram for the different flow topologies. The richness of the problem is best illustrated by the fact that sixteen different topologies appeared at different regime parameters of the flow. In spite of the topological complexity, and since the basic change in flow topology from a flow without bubbles to a flow with a re-circulating bubble cannot be explained as an instability, the basic mechanisms of the early transition still need to be clarified. For this reason we restrict the analysis to a configuration in which swirl is generated by rotating the top and the bottom lid with the same rotational speed, with parameters set to values corresponding to the axisymmetric regime where the first re-circulating bubble appears.

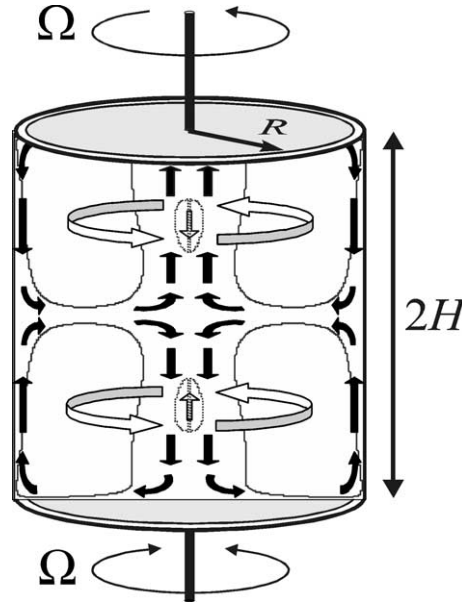


Fig. 1. Sketch of the flow domain.

## 2. Formulation of the problem

Consider a viscous, incompressible, axisymmetric flow in a cylinder of height  $2H$  and radius  $R$  (Fig. 1). The bottom and top covers rotate with constant angular velocities  $\Omega_1$ ,  $\Omega_2$ , respectively. Three dimensionless numbers characterizing the problem are the Reynolds number,  $Re = \Omega_1 R^2/\nu$ , where  $\nu$  is the kinematic viscosity of the fluid; the aspect ratio,  $h = H/R$ , and the ratio of angular velocities,  $\gamma = \Omega_2/\Omega_1$ .

The flow is described using cylindrical coordinates  $(r, \theta, z)$  with corresponding velocity  $\mathbf{u} = (u_r, u_\theta, u_z)$  and vorticity  $\boldsymbol{\omega} = (\omega_r, \omega_\theta, \omega_z)$  that only depend on  $r$  and  $z$ . We introduce a  $rz$ -plane analogous of the stream function,  $\psi$ , and a local circulation,  $ru_\theta$ , as follows:

$$u_r = \frac{\partial \psi}{r \partial z}, \quad u_z = -\frac{\partial \psi}{r \partial r}. \quad (1)$$

$$\omega_r = -\frac{\partial(ru_\theta)}{r \partial z}, \quad \omega_z = \frac{\partial(ru_\theta)}{r \partial r}. \quad (2)$$

Hence, the velocity and vorticity fields can be described by the scalar function  $\psi$  and the azimuthal components of velocity  $u_\theta$  and vorticity  $\omega_\theta$ . Formulated in these variables [11] the system is governed by the two transport equations

$$\frac{\partial u_\theta}{\partial t} + \frac{\partial(u_r u_\theta)}{\partial r} + \frac{\partial(u_z u_\theta)}{\partial z} - \frac{2u_r u_\theta}{r} = \frac{1}{Re} \left[ \frac{\partial}{\partial r} \left( \frac{\partial(ru_\theta)}{r \partial r} \right) + \frac{\partial^2 u_\theta}{\partial z^2} \right], \quad (3)$$

$$\frac{\partial \omega_\theta}{\partial t} + \frac{\partial(u_r \omega_\theta)}{\partial r} + \frac{\partial(u_z \omega_\theta)}{\partial z} - \frac{\partial(u_\theta^2)}{r \partial z} = \frac{1}{Re} \left[ \frac{\partial}{\partial r} \left( \frac{\partial(r\omega_\theta)}{r \partial r} \right) + \frac{\partial^2 \omega_\theta}{\partial z^2} \right], \quad (4)$$

and the Poisson equation

$$\frac{\partial^2 \psi}{\partial z^2} + \frac{\partial^2 \psi}{\partial r^2} - \frac{\partial \psi}{r \partial r} = r\omega_\theta. \quad (5)$$

The equations are put into non-dimensional form by scaling length and time with  $R$  and  $\Omega_1$ , respectively. The advantage of this formulation, as compared to the one of primitive variables, is that the pressure is eliminated and that the continuity equation is automatically satisfied. Boundary conditions are established from the no-slip assumption of the velocity. For the numerical simulation we use the finite difference code developed at LIMSI/CNRS [11,12]. The transport equations (3) or (4) are discretized by a second-order central difference scheme and the Poisson equation (5) is discretized to fourth-order accuracy using three-point expressions for the derivatives. Previous comparisons of numerical results and experiments for the configuration with a fixed cover ( $\gamma = 0$ ) showed that simulations with a grid size of  $100 \times 100h$  mesh points for  $h \geq 1$  and  $100/h \times 100$  mesh

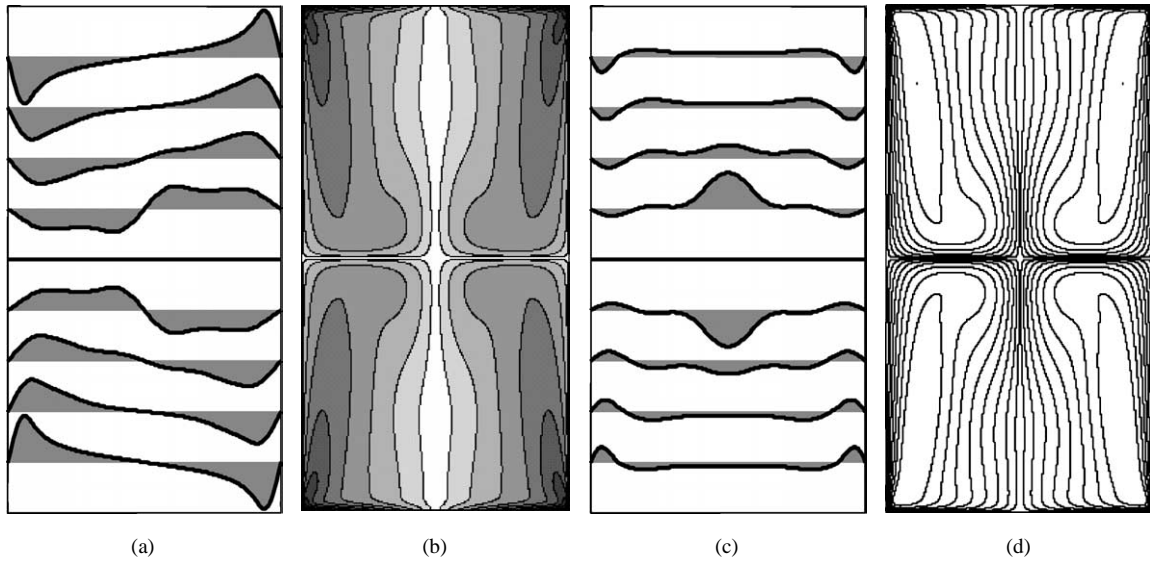


Fig. 2. Features of flow in meridional intersection for cylinder with  $h = 1$  and counter-rotation top and bottom at  $Re = 2000$ . (a) Profile of azimuthal velocity; (b) Contours of vortex surface; (c) Profile of axial velocity; (d) Contours of stream surface.

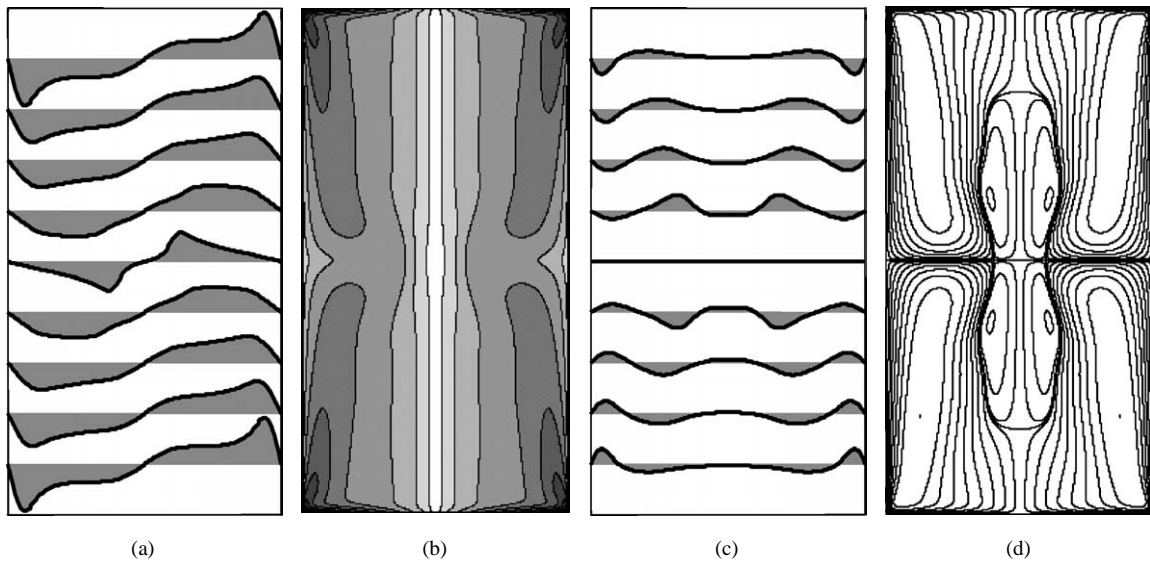


Fig. 3. Features of flow in meridional intersection for cylinder with  $h = 1$  and co-rotating top and bottom at  $Re = 2000$ . (a) Profile of azimuthal velocity; (b) Contours of vortex surface; (c) Profile of axial velocity; (d) Contours of stream surface.

points for  $h < 1$  correctly predict the onset of the reverse flow within experimental accuracy. For further information about the computing code and the implementation of boundary conditions, see Refs. [11,12,26].

In the present study we have investigated the particular case where the end covers either co- or counter-rotate with identical and constant angular velocity ( $\gamma = \pm 1$ ). Characteristic properties of counter-rotation are shown in Figs. 2(a)–2(d), while characteristics of co-rotation are depicted in Figs. 3(a)–3(d). At counter-rotation, the axial and azimuthal velocities are equal to zero at the middle plane (see Figs. 2(a) and 2(c)). The pumping in this case leads to the formation of a purely progressive motion along the cylindrical axis towards the disks (Fig. 2(c)). In Fig. 2(d), contours of the stream-surfaces are in the meridional intersection seen as two mirror images, consisting of closed and deformed tori. In Figs. 2 and 3, the intensity levels of stream

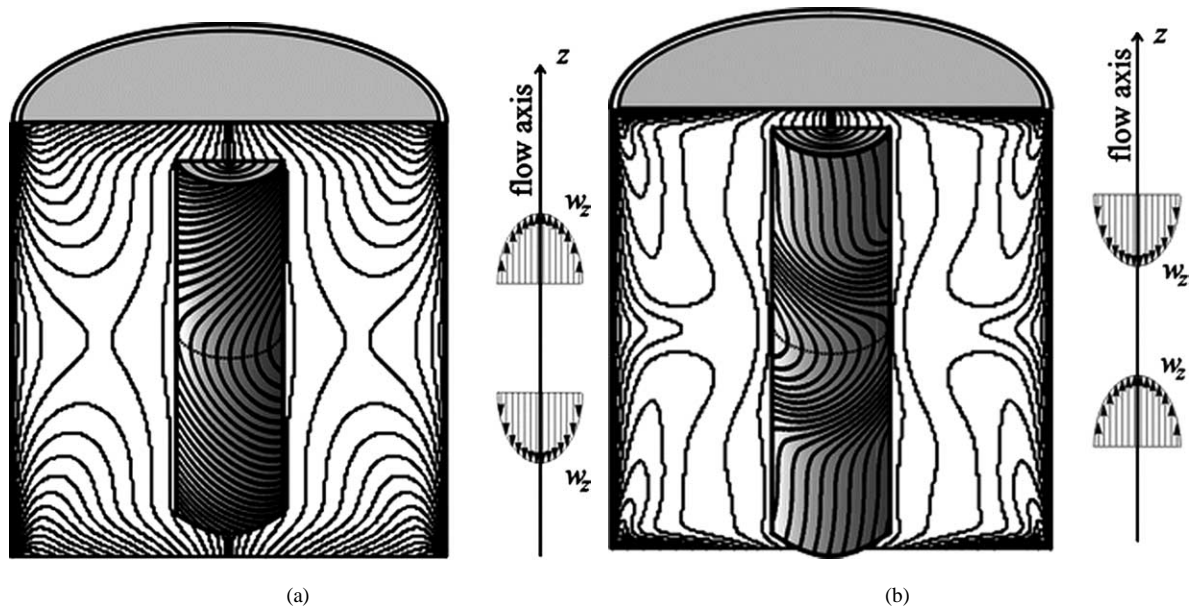


Fig. 4. Contours of vortex surface in meridional intersection, structure of vortex lines on central vortex tube, and axial velocity profile induced by central vortex system in a cylinder with  $h = 1$  and co-rotating top at bottom at (a)  $Re = 150$  and (b)  $Re = 1300$ .

surfaces and circulation (referred to as vortex tubes or vortex surfaces) in the meridional intersection are non-uniformly spaced, with different numbers  $n$  of the levels determined by

$$\text{const}_i = \min(B) + [\max(B) - \min(B)] \times (i/n)^3,$$

where  $B$  is  $\psi$  or  $ru_\theta$ . Profiles of the vortex-surfaces are two mirrored sets from deformed semitorus, which encloses each other and break into disks (Fig. 2(b)). Such a semi-torus of the vortex tube is similar to a vortex semi-ring resting on a disk surface. Please note that the vortex rings only can induce a purely progressive motion along the axis toward the disks, whereas they are not capable of generating re-circulating bubbles.

In the case of co-rotating disks, another flow picture is obtained (see Figs. 3(a)–3(d)). Here the azimuthal velocities are non-zero in the middle cross-section, and the fluid co-rotates in the upper and the lower half part of the cylinder (Fig. 3(a)). Contours of the stream-surfaces in the meridional intersection (Fig. 3(d)) show the appearance of symmetrical bubbles, i.e. recirculation zones with weak reverse flow along the cylindrical axis (Fig. 3(c)). In this case the vorticity distribution is easy to describe (see Fig. 3(b)). Paraxial vortex tubes akin to enclosed cylinders pass through the whole flow domain in the central part of the flow and structures of semi-torus shape are located near the cylindrical wall. Pronounced longitudinal vortex structures appear near the flow axis. In the following we analyze the influence from the torsion of these longitudinal vortices on the bubble generation. The iso-curves of  $\psi$  and  $ru_\theta$ , computed from Eqs. (1)–(5), are defined as the intersection of the axisymmetric stream surfaces and vortex surfaces, respectively, with any meridional plane. Even though the surfaces are axisymmetric, the streamlines and vortex lines are three-dimensional. This is illustrated in Fig. 4 that shows that even when the longitudinal vortex tubes are pure axisymmetric they consist of real three-dimensional helical-like vortex lines with non-zero torsion or local helical pitch.

### 3. Right- and left-handed symmetry of the vortex lines

To determine the induced axial flow in swirl flows the three-dimensional structure of the vortex lines is of fundamental importance. The difference between vortex lines with right- and left-handed helical symmetry is of special interest as the sign of local torsion or helical pitch determines the sign of the induced axial velocity (positive pitch defines a right-handed helical vortex structure and negative pitch a left-handed one). Recent progress in the study of the vortex structures has revealed that there exists a direct relation between the type of vortex symmetry and the appearance of swirl flow with jet-like or wake-like velocity profiles [3–6]. To illustrate this, consider the change in the velocity profile during vortex breakdown of an axial slender vortex in a swirl tube. The experimental velocity profiles before and after breakdown are usually analyzed using the empirical relations [1,2],

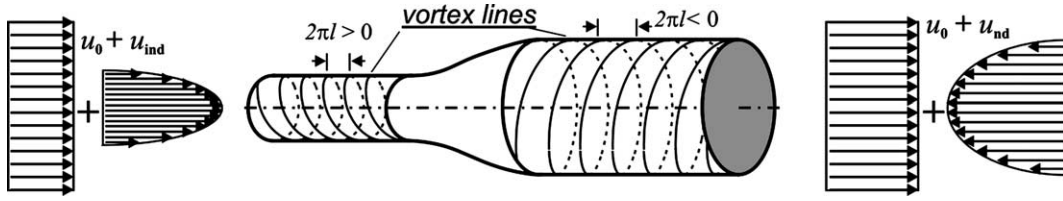


Fig. 5. Sketch of the structure of vortex lines in slender vortices before and after breakdown in swirl tube flows, and axial velocity profiles –  $u_{\text{ind}}$  induced by both vortex systems with profiles of additional transversal fluid motion –  $u_0$ .

$$\begin{aligned} u_\theta &= \frac{K}{r} (1 - \exp(-\alpha r^2)), \\ u_z &= W_1 + W_2 \exp(-\alpha r^2) = W_1 + W_2 - W_2 (1 - \exp(-\alpha r^2)), \end{aligned} \quad (6)$$

where  $K$ ,  $W_1$ ,  $W_2$ ,  $\alpha$  are empirical constants. The relations (6) correspond to the analytical solution of the Euler equations,

$$u_\theta = \frac{\Gamma}{2\pi r} [1 - \exp(-r^2/\varepsilon^2)], \quad u_z = u_0 - \frac{\Gamma}{2\pi l} [1 - \exp(-r^2/\varepsilon^2)], \quad (7)$$

for a velocity field induced by a columnar helical vortex consisting of three-dimensional helical vortex lines of constant pitch  $2\pi l$ . The corresponding vorticity distribution in the vortex core is given as

$$\omega_z = \omega_\theta l/r = \Gamma \exp(-r^2/\varepsilon^2)/\pi \varepsilon^2 \quad \text{and} \quad \omega_r = 0, \quad (8)$$

where  $\varepsilon$  is the length scale of the vortex core and the radial vorticity component is zero because of the cylindrical form of the vortex surface. Comparing the exact solution (7) with the empirical formulae (6) yields,

$$\Gamma = 2\pi K, \quad l = K/W_2, \quad u_0 = W_1 + W_2, \quad \varepsilon = 1/\sqrt{\alpha}. \quad (9)$$

These formulas give the physical interpretation of the empirical constants and show that a change from a jet-like to a wake-like axial velocity profile is associated with a change in the sign of  $W_2$  and hereby with a change in the sign of the helical pitch. Fig. 5 illustrates how the vortex lines in the columnar vortices before and after breakdown are associated with a change in helical pitch, from a right-handed structure to a left-handed one. Further it shows that the corresponding axial velocity profiles consist of a constant axial velocity  $u_0$ , superposed by a jet-like or a wake-like velocity profile  $u_{\text{id}}$ . Upstream the breakdown zone the positive helical pitch induces a jet-like profile and downstream a wake-like profile is induced. This is further confirmed by the studies of Okulov and co-workers [3–5], who demonstrated that both left-handed and right-handed vortex structures may exist under the same integral flow parameters and that there is a good agreement between measurements and analytical results using the concept of helical symmetry. This implies that vortex breakdown of longitudinal vortices may be considered as a transition between different types of helical vortex symmetry.

The theory developed in [3–5], however, only describes the features of the flow before and after vortex breakdown, and it does not show how the helical symmetry of the vorticity field changes during breakdown, when changing the governing model parameters, and how it relates to the generation of re-circulating bubbles. Obviously, the helical pitch changes continuously when changing the model parameters. Thus, a positive value of the helical pitch before breakdown will continuously be transformed into a negative value after breakdown. As a measure of the transitional properties of the vortex lines during vortex breakdown, we introduce the dimensionless local helical pitch, defined in each point along the vortex tube,

$$p = 2\pi \frac{l}{r} = 2\pi \frac{\tau}{\kappa}, \quad (10)$$

where  $r$  is the local radius of the vortex tube and  $l$  is the local pitch of the vortex line, with local values of curvature  $\kappa = r/(r^2 + l^2)$  and torsion  $\tau = l/(r^2 + l^2)$ .

In the present case of a cylindrical cavity with co-rotating lids a pronounced longitudinal vortex structure is formed along the axis, hence making it an ideal case for studying transitional properties of paraxial vortices. Because the rotational speed of the two lids is identical the middle plane ( $z = 0$ ) forms a symmetry boundary between the two half-planes. For this reason only the upper half part of the cylinder will be considered in the following. To understand how the concept of transition of helical symmetry works, assume that the disk rotates in the positive direction of the azimuthal coordinate. Then, if a right-handed helical vortex is created, a jet-like profile induces an additional velocity component along the cylindrical axis that pumps fluid towards the rotating disk (see Fig. 4(a)). Changing the helical symmetry to a left-handed helical vortex (Fig. 4(b)) induces an additional wake-like profile that tends to diminish the axial velocity component, leading to evanescence of the fluid motion at the cylindrical axis and to the appearance of reversal flows.

Because of the symmetry the local helical pitch becomes infinity at the symmetry plane ( $z = 0$ ). To avoid this, instead of the helical pitch we employ the dimensionless twist of the vortex lines,  $\kappa/\tau = r/l$ , as main parameter for studying the helical

properties during vortex breakdown. This parameter is inversely proportional to the pitch and becomes zero at the symmetry plane. In the case of a pure cylindrical vortex surface the parameter has a simple geometrical interpretation as the tangent of the angle of inclination,  $\beta$ , between the vorticity vector and the axial direction. Ignoring the thin Ekman-type boundary layer on the rotating disk, the considered vortex structures are very close to be of pure cylindrical form, as will be shown in the following. Thus, as a good approximation, the dimensionless twist of the helix-like vortex structures is computed as

$$\frac{\kappa}{\tau} = \frac{r}{l} \approx \frac{\omega_\theta}{\omega_z} = \tan \beta.$$

Scaling the twist parameter to the specific geometry of the cavity, in dimensionless form we get the following expression,

$$\mathbf{K} = \frac{R}{pH} \approx \frac{R}{2\pi H} \frac{\omega_\theta}{\omega_z} = \frac{R}{2\pi H} \tan \beta.$$

Using the definitions given above, the geometrical structure of the vortex lines may be analyzed simply by utilizing the distribution of the vorticity components as a measure of the pitch or twist. As this approximation is based on the assumption that the vortices form cylindrical surfaces, it cannot be used to analyze vortex structures with sizable deformed surfaces, such as the structures of semi-torus shape located near the cylindrical wall. On the other hand, using the vorticity components to identify geometrical parameters, such as pitch and twist, greatly simplifies the analysis of longitudinal vortex structures. In this connection it should be noted that the idea of analyzing vortex breakdown using vorticity field transformations is not new. In various numerical studies on vortex breakdown (e.g. [13,16,30]) the distribution of circumferential vorticity has been used as a main parameter, and in [29] a feedback mechanism based on the redistribution from axial to circumferential vorticity was used to explain the initiation of bubble-type breakdown of swirl flows in tubes. However, using the concept of helicity of the vortex lines as a main parameter for studying vortex breakdown is new and the primary objective of the present work. In the next section we analyze the influence of changes in helical symmetry and twist of vortex lines to define conditions for vortex breakdown and the appearance of re-circulating bubbles.

#### 4. Results and discussion

To cover a broad range of parameter values, the flow was computed at three aspect ratios,  $h = 1, 1.5$ , and  $2$ , and at several Reynolds numbers, starting with a basic flow topology without re-circulating bubbles. In accordance with the bifurcation diagram of flow patterns [27], the studied flow regime lies in the domain where the basic change of the flow topology is characterized by the appearance of a single axial re-circulation zone with a weak reverse flow along the cylindrical axis.

In order to simplify the comparison of flow patterns and vortex characteristics the results are presented in tables. The first column of the tables gives the meridional intersection of the vortex structures of the central vortex tube, marked by different line types. Here a thin solid line designates the surface of the vortex structure near the axis, whereas a thick solid line shows the location of the outer surface of the longitudinal vortex structure. In between the two solid lines, dashed and dotted lines show the distribution of the vortex surfaces. The second column shows the variation of the twist parameter  $\mathbf{K}$  along vortex tubes, designated by the same type of lines. The last two columns depict the changes in flow pattern by showing axial velocity profiles and streamlines in a meridional intersection, respectively.

Three different flow regimes are shown in the tables. In Table 1 is shown flow cases that in a ( $Re$ - $h$ ) topology diagram is located in regions without re-circulating bubbles. Table 2 presents results from computations close to bubble generation, and in Table 3 is shown results from computations in which re-circulating bubbles are generated. At the lowest Reynolds numbers (Table 1) the flow regimes indicate the existence of a right-handed helical vortex ( $p$  and  $\mathbf{K}$  positive) in the upper half part of the cylinder. Please note that, as seen from the rotating disks, the flow in the lower half part is identical to the one in the upper half part. For the flow cases treated in Table 1 jet-like profiles of axial velocity, pointing towards the rotating disks, are formed as a superposition of the central vortex structure and the peripheral deformed vortex semi-rings. By increasing  $Re$  one can observe a transition from a right-handed to a left-handed helix-like symmetry in the upper half part of the cylinder ( $p$  and  $\mathbf{K}$  now become negative). In Table 2 this observation is demonstrated for flows where a bubble is just about to be formed. The change in helical symmetry leads to the appearance of a dent in the jet-like profiles of the axial velocity. At increasing Reynolds numbers (Table 3) the twist parameter  $\mathbf{K}$  and the size of the dent increases further, resulting in flow reversal at the center axis. It is noteworthy that, independent of aspect ratio and Reynolds number, the appearance of flows with jet-like profiles is always associated with a change in helical symmetry of the central vortex structure (from right-handed to left-handed) and that the value of the twist parameter at the point where flow reversal takes place is given as (approximately)

$$\mathbf{K} \approx 0.6 \quad \text{or} \quad \min(p) \approx R/0.6H.$$

Since this was observed for all the computed flow cases we take it as a necessary, but not sufficient, condition that the creation of a re-circulating bubble is associated with a change in helical symmetry of the central vortex structure and that the twist

Table 1

Vortex structure and flow pattern for flows at Reynolds numbers without bubbles

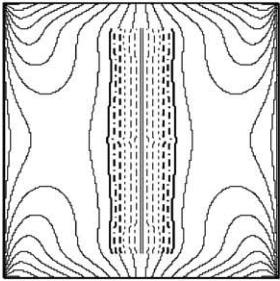
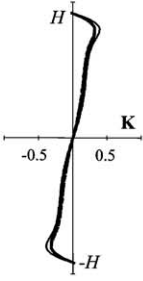
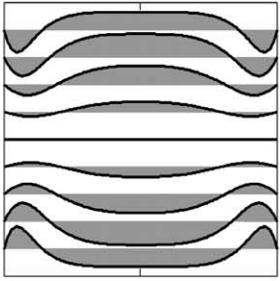
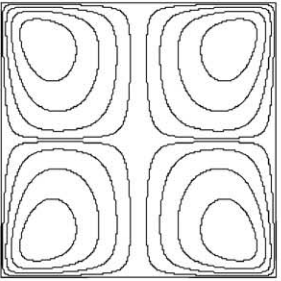
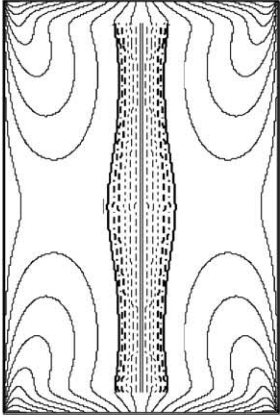
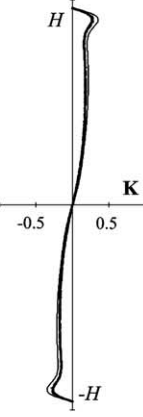
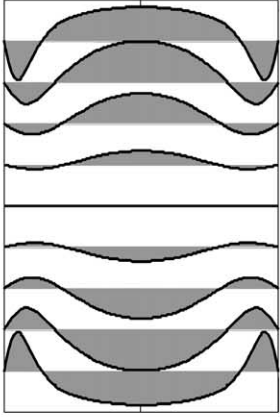
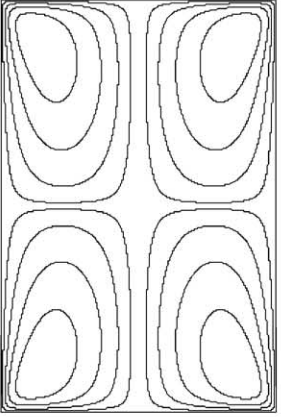
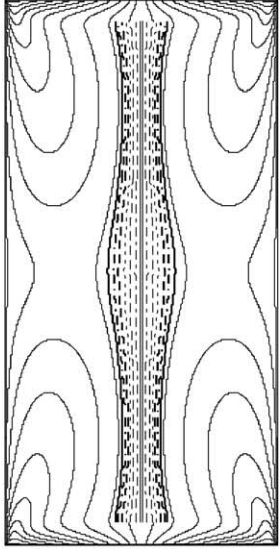
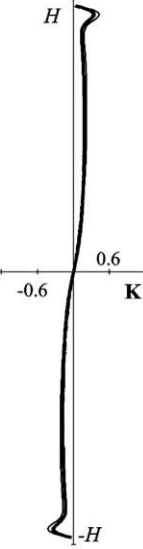
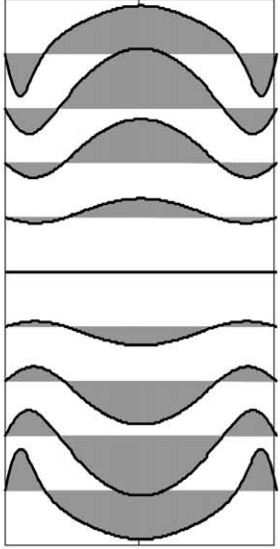
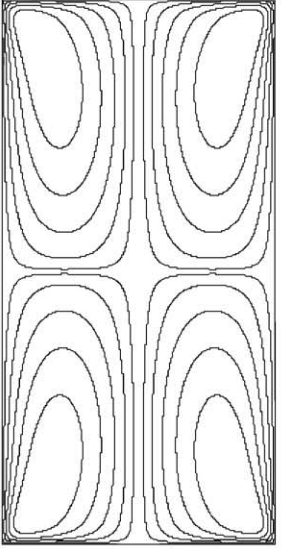
	Profiles of the vortex tubes	Twist of vortex lines	Profiles of the axial velocity	Profiles of the stream tubes
<b>Re = 150, <math>h = 1</math></b>				
<b>Re = 300, <math>h = 1.5</math></b>				
<b>Re = 500, <math>h = 2</math></b>				



Table 2

Vortex structure and flow pattern for flows at Reynolds numbers close to bubble generation

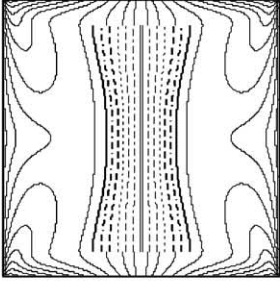
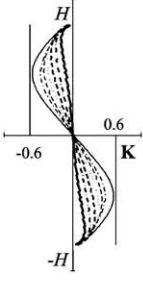
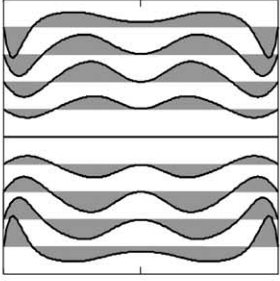
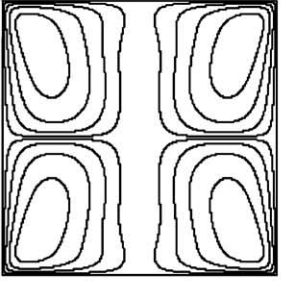
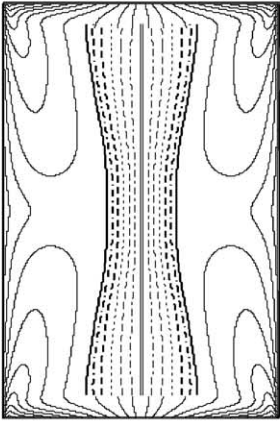
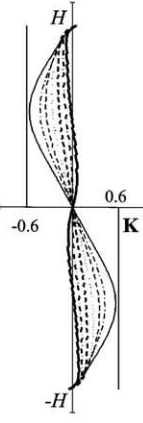
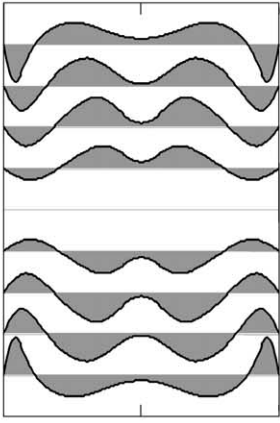
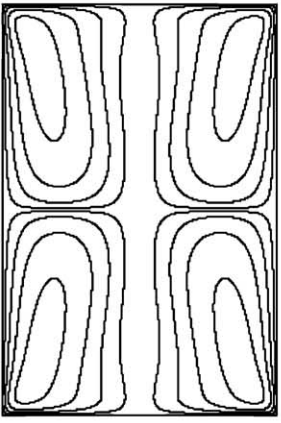
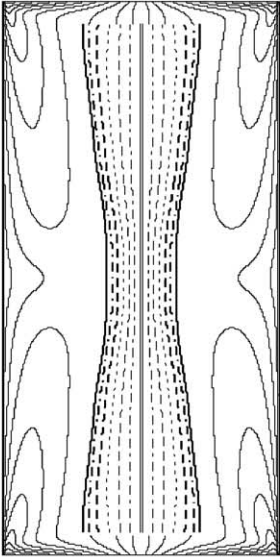
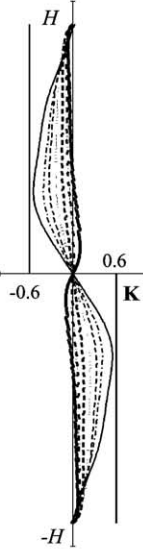
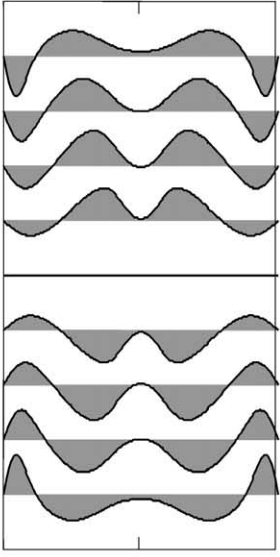
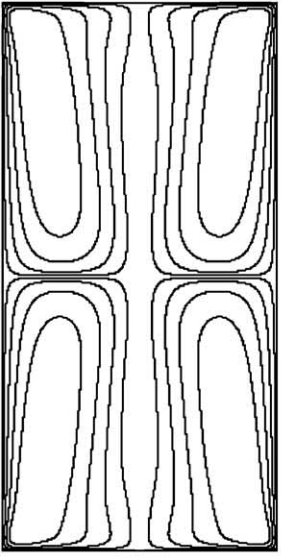
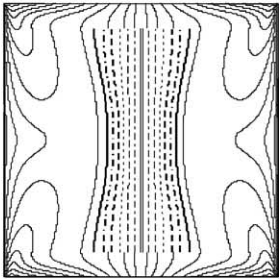
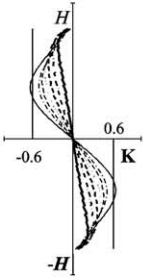
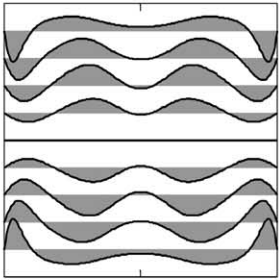
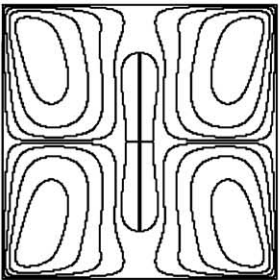
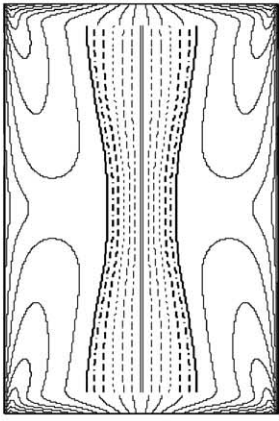
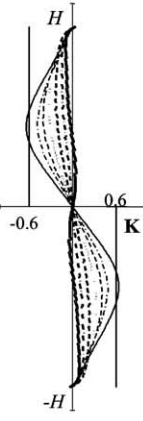
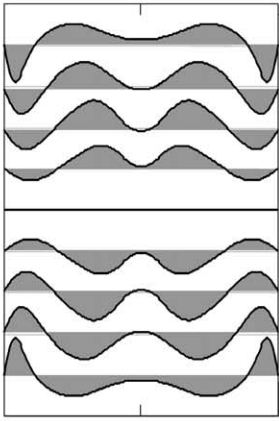
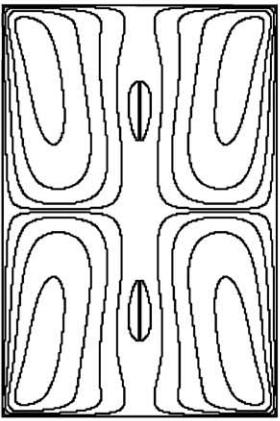
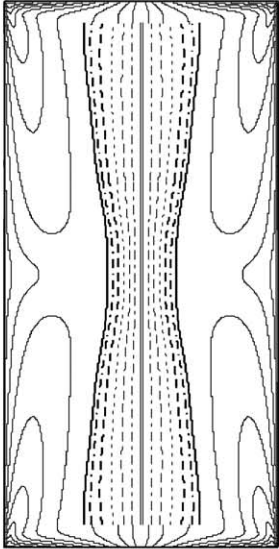
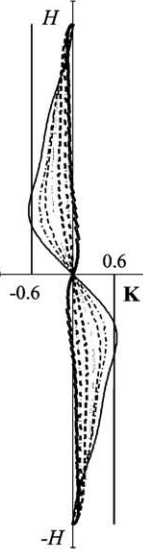
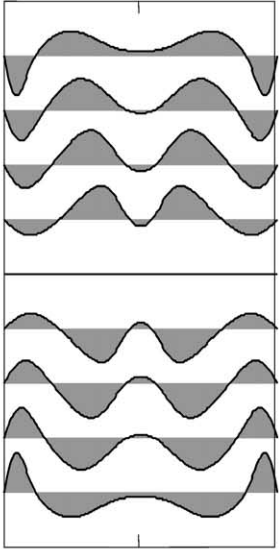
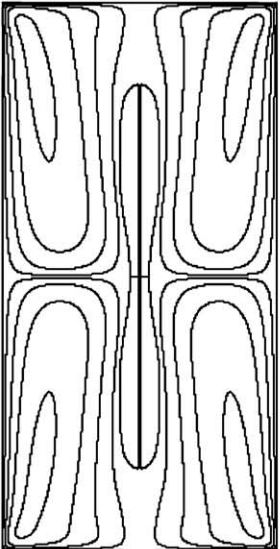
	Profiles of the vortex tubes	Twist of vortex lines	Profiles of the axial velocity	Profiles of the stream tubes
<b>Re = 450, <math>h = 1</math></b>				
<b>Re = 700, <math>h = 1.5</math></b>				
<b>Re = 1100, <math>h = 2</math></b>				

Table 3

Vortex structure and flow pattern for flows at Reynolds numbers at which a re-circulating bubble is present

	Profiles of the vortex tubes	Twist of vortex lines	Profiles of the axial velocity	Profiles of the stream tubes
<b>Re = 500, <math>h = 1</math></b>				
<b>Re = 750, <math>h = 1.5</math></b>				
<b>Re = 1200, <math>h = 2</math></b>				

parameter at the point where flow reversal is initiated attains a value  $\mathbf{K} \cong 0.6$ . Furthermore, this seems to be a threshold value that only can be attained at the center axis inside a re-circulating bubble.

## 5. Conclusions

In this study numerical solutions of the axisymmetric Navier–Stokes equations were used to examine changes in the helical symmetry of vortex lines for the case of a steady swirl flow in a cylinder with co-rotating top and bottom.

The computed results demonstrate that the change in axial velocity distribution from a jet-like profile to a wake-like during vortex breakdown may be explained as a transition from right- to left-handed helical symmetry of the vorticity field. As a main result, it is found that a necessary condition of flow reversal or vortex breakdown is the existence of a left-handed helical vortex. Indeed, only a left-handed helical vortex structure can induce a wake-like axial velocity profile and, hence, it is a necessary prerequisite for flow reversal in swirl flows.

The computations show that symmetry changes take place at increasing Reynolds numbers and that flow reversal on the center axis is associated with a growth of the twist parameter of the vortex lines. For all studied flow cases, independent of aspect ratio and Reynolds number, it was observed that the twist parameter of the central vortex attains a value of  $\mathbf{K} \cong 0.6$  at the point where flow reversal takes place and that this is a threshold value that is not exceeded in any other part of the flow.

Thus, the hypothesis that the change in axial velocity distribution from a jet-like profile to a wake-like during vortex breakdown is associated with a transition of the helical symmetry in the central vortex structure has been supported by the analyzed results of a swirl flow in a closed cylinder with co-rotating top and bottom.

## Acknowledgements

This research has been supported in part by the INTAS (grant no. 00-00232) and RFBR (grant no. 01-01-00899), and the Otto Mønsted Foundation.

## References

- [1] S. Leibovich, The structure of vortex breakdown, *Annu. Rev. Fluid Mech.* 10 (1978) 221–246.
- [2] M.P. Escudier, Vortex breakdown: observations and explanations, *Prog. Aerospace Sci.* 25 (1988) 189–229.
- [3] V.L. Okulov, The transition from the right helical symmetry to the left symmetry during vortex breakdown, *Tech. Phys. Lett.* 22 (10) (1996) 798–800.
- [4] T. Murakhtina, V. Okulov, Modelling of the turbulent vortex breakdown as a transition from column to conical helical vortices, in: S. Dopazo (Ed.), *Advance in Turbulence*, vol. 8, Barcelona, 2000, pp. 817–820.
- [5] S. Martemianov, V.L. Okulov, On heat transfer enhancement in swirl pipe flows, *Int. J. Heat Mass Transfer* 47 (2004) 2379–2393.
- [6] S.V. Alekseenko, P.A. Kuibin, V.L. Okulov, S.I. Shtork, Helical vortices in swirl flow, *J. Fluid Mech.* 382 (1999) 195–243.
- [7] H.U. Vogel, Experimentelle Ergebnisse über die laminare Strömung in einem zylindrischen Gehäuse mit darin rotierender Scheibe, Max-Planck-Institut für Strömungsforschung, Göttingen, 1968, Bericht 6.
- [8] B. Ronnenberg, Ein selbstjustierendes 3-Komponenten-Laserdoppleranemometer nach dem Vergleichsstrahlverfahren, angewandt auf Untersuchungen in einer stationären zylinder-symmetrischen Drehströmung mit einem Rückströmgebiet, Max-Planck-Institut für Strömungsforschung, Göttingen, 1977, Bericht 19.
- [9] M.P. Escudier, Observations of the flow produced in cylindrical container by a rotating endwall, *Exp. Fluids* 2 (1) (1984) 189–196.
- [10] K.G. Roesner, Recirculation zones in a cylinder with rotating lid, in: A. Tsinober, H.K. Moffat (Eds.), *Proceeding of the IUTAM Symposium on Topological Fluid Mechanics*, University of Cambridge Press, Cambridge, 1989.
- [11] O. Daube, Numerical simulation of axisymmetric vortex breakdown in a closed cylinder, *Lectures in Appl. Math.* 308 (1991) 131–152.
- [12] J.N. Sørensen, T.P. Loc, High-order axisymmetric Navier–Stokes code: description and evaluation of boundary condition, *Int. J. Numer. Methods Fluids* 9 (1989) 1517–1537.
- [13] J.M. Lopez, Axisymmetric vortex breakdown: Part 1. Confined swirling flow, *J. Fluid Mech.* 221 (1990) 533–552.
- [14] N. Tsiverblit, Vortex breakdown in cylindrical container in the light of continuation of a steady solution, *Fluid Dyn. Res.* 11 (1993) 19–35.
- [15] H.M. Blackburn, J.M. Lopez, Modulated rotating waves in an enclosed swirling flow, *J. Fluid Mech.* 465 (2002) 33–58.
- [16] J.M. Lopez, A.D. Perry, Axisymmetric vortex breakdown. Part 3. Onset of periodic flow and chaotic advection, *J. Fluid Mech.* 234 (1992) 449–471.
- [17] J.N. Sørensen, E.A. Christensen, Direct numerical simulation of rotating fluid flow in a closed cylinder, *Phys. Fluids* 7 (4) (1995) 764–778.
- [18] A.Y. Gelfgat, P.Z. Bar-Yoseph, A. Solan, Three-dimensional instability of axi-symmetric flow in rotating lid-cylinder enclosure, *J. Fluid Mech.* 438 (2001) 363–377.
- [19] A. Spohn, M. Mory, E.J. Hopfinger, Experiments on vortex breakdown in a confined flow generated by a rotating disk, *J. Fluid Mech.* 370 (1998) 73–99.

- [20] F. Sotiropoulos, Y. Ventikos, The three-dimensional structure of confined swirling flows with vortex breakdown, *J. Fluid Mech.* 426 (2001) 155–175.
- [21] Y. Ventikos, The effect of imperfections on the emergence of three-dimensionality in stationary vortex breakdown bubbles, *Phys. Fluids* 14 (3) (2001) L13–L16.
- [22] V.L. Okulov, A.A. Dekterev, Alteration in the symmetry of the vorticity field during the vortex breakdown in a closed cylinder with a rotating endwall, *Thermophys. & Aeromech.* 5 (1) (1998) 119–122.
- [23] D.T. Valentine, C.C. Jahnke, Flows induced in cylinder with both end walls rotating, *Phys. Fluids* 6 (1994) 2702–2710.
- [24] A.Y. Gelfgat, P.Z. Bar-Yoseph, A. Solan, Steady states and oscillatory instability of swirling flow in cylinder with rotating top and bottom, *Phys. Fluids* 8 (10) (1996) 2614–2625.
- [25] J.F. Pinton, F. Chilla, N. Mordant, Intermittency in the closed flow between coaxial corotating disks, *Eur. J. Mech. B Fluids* 17 (4) (1998) 535–547.
- [26] M. Brøns, L.K. Voigt, J.N. Sørensen, Streamline topology of steady axisymmetric vortex breakdown in cylinder with co- and counter-rotating end-covers, *J. Fluid Mech.* 401 (1999) 275–292.
- [27] M. Brøns, L.K. Voigt, J.N. Sørensen, Topology of vortex breakdown bubbles in cylinder with rotating bottom and free surface, *J. Fluid Mech.* 428 (2001) 133–148.
- [28] M. Brøns, Topological fluid mechanics of axisymmetric flows, in: J.N. Sørensen, E.J. Hopfinger, N. Aubry (Eds.), *Simulation and Identification of Organized Structures in Flows*, Kluwer Academic, 1999, pp. 213–222.
- [29] W. Althaus, Ch. Brückner, M. Weimer, Breakdown of slender vortices, in: S.I. Green (Ed.), *Fluids Vortices*, Kluwer Academic, 1995, pp. 373–426.
- [30] G.L. Brown, J.M. Lopez, Axisymmetrical vortex breakdown: Part 2. Physical mechanisms, *J. Fluid Mech.* 221 (1990) 553–576.